1. INTRODUCTION

1.1 Definition of corrosion

Corrosion can be defined as "an unwanted chemical attack of a metal by its environment". Corrosion is an electrochemical process, involving metals and electrolytes [1]. All corrosion reactions obey the thermodynamic laws. With the exception of noble metals like gold and platinum all other metals corrode and transform into substances similar to their mineral ores from which they are extracted. It is important to note that, the advanced countries are reported to be suffering an annual loss equivalent to 2-4% of their GNP due to corrosion [2]. Nearly 20-25% of this value could be avoided by using appropriate anticorrosion technology. Many preventive measures are used against metallic corrosion.

1.2 Electrochemical theory of corrosion

Generally, corrosion in acidic media involves the formation of hydrogen gas at the cathode and metal dissolution at the anode as:

$M \longrightarrow M^{2+} + 2e$ anodic reaction (oxidation) (1.1)

$2H^{+} + 2e \longrightarrow H_2$ cathodic reaction (reduction) (1.2)

The other possible cathodic reaction is

$O_2 + 4H^{+} + 4e \longrightarrow 2H_2O$ reduction of oxygen (1.3)

In neutral and alkaline solutions, the cathodic reaction is oxygen reduction as:

$2H_2O + O_2 + 4e \longrightarrow 4OH^{-}$ (1.4)

The tendency of a metal to corrode may be assessed by "the amount of energy liberated in the change from the metallic state to the oxidized state" or in electrochemical terms by "the standard electrode potential of the metal". The metals are arranged in an order of their standard electrode potential. The noble metals appear at the noble end and the more reactive metals at the active end of the series.

1.3 Polarization

The extent of potential change caused by the flow of current from an electrode is called polarization. There are three types of polarization which mainly, concentration polarization, activation polarization and resistance polarization

1.3.1 Concentration polarization

According to the Nernst equation, the potential of an electrode depends upon the concentration of ions in the electrolyte in its immediate vicinity. In the absence of an external current, the Nernst equation is:

$$E_1 = E_1^o + \frac{0.059}{n} \log a_{M^{+n}} \qquad (1.5)$$

If an external current is applied, the concentration of the M^{+n} ions in the solution near the electrode increases by ionic diffusion and convection migration. Only the last type can be controlled. At higher currents, the potential (E_2) of the electrode is given by:

$$E_2 = E_2^o + \frac{0.059}{n} \log a_{M_s^{+n}} \qquad (1.6)$$

The difference in potential (E_2-E_1) is known as concentration polarization and is given by:

$$\varepsilon = E_2 - E_1 = \frac{0.059}{n} \log \frac{a_{M^{+n}}}{a_{M_s^{+n}}} \qquad (1.7)$$

1.3.2 Activation polarization

Activation polarization is caused by a slow electrode reaction. In this case some activation energy is required to start the reaction on the surface of electrode. An example is the reduction of hydrogen ions on the cathode surface.

$$2H^+ + 2e \longrightarrow H_2 \qquad (1.8)$$

1.3.3 Resistance polarization

It is an ohmic drop (iR) through either a portion of the electrolyte surrounding the electrode or through a metal reaction product film on the surface or both, where (i) is the current density and (R) is the value of the path resistance in ohms.

1.4 Types of corrosion

Corrosion can be divided into three categories [3, 4] as follow:

1.4.1 Corrosion distinguished by the naked eye.

1.4.1.1 General corrosion

This type of corrosion occurs over the whole or most of the exposed surface of a material. Because of the uniform nature of the general corrosion a "corrosion allowance" can be added to design thickness of the vessel or piping

in many instances to provide for an expected service life. There are three groups or classifications for acceptable corrosion rates depending on the applications as follow [5]:

- < 0.005 ipy (< 5 mpy) good corrosion resistance.
- 0.005 to 0.05 ipy (5 to 50 mpy) piping, valve bodies, vessels ...etc.
- > 0.05 ipy (> 50 mpy) not considered for use in the application.

1.4.1.2 Localized corrosion.

It is the type of corrosion covers only a fraction of the total surface area such as pitting and crevice corrosion.

(I)Pitting corrosion.

It is one of the most destructive and insidious forms [6, 7], as the attack is extremely localized resulting holes in metals and causing the equipment failure. The term pitting factor is used to express the ratio of the depth of the deepest pit to the average penetration calculated from weight loss. Pitting is generally associated with halide ions and hydrochlorides. Stainless steel in aqueous solutions containing chlorides will be subjected to pitting corrosion. A clean, smooth metal surface will be more resistant to this type of attack. Also, the addition of inhibitors to the solution will occasionally reduce or prevent pitting.

(II) Crevice corrosion.

It is the type of localized corrosion in which the faying surface become depleted of oxygen which adjacent areas are cathodic because of ready access of depolarizing species [7]. The most important examples of this type are fibrous gaskets, alloys which depend on oxide films for corrosion resistance and also stainless steels.

1.4.1.3 Galvanic corrosion.

It is a bimetallic corrosion [7]. When one metal is electrically coupled to another metal or nonmetal in an electrically conducting environment, the more anodic member of the galvanic couple corrodes more rapidly than the other cathodic member, which is protected cathodically. Insulating dissimilar metals from each other can prevent this type of corrosion.

1.4.1.4 Velocity-related corrosion.

Erosion and cavitation corrosions are the two forms of velocity-related phenomena [7]. Fretting is also corrosion of this type which is caused between two rubbing metallic surfaces while simultaneously exposed to a corrosive environment.

(I) Erosion corrosion.

This type of corrosion occurs when the protective films are mechanically removed by the action of flowing fluids environment.

(II) Cavitation.

This type occurs when the conditions of the liquid flow can set up low-pressure areas between the metal and environment such as when liquid vaporizes and forms bubbles.

1.4.2 Corrosion recognized with the assistance of certain supplementary means of examination.

1.4.2.1 Intergranular corrosion.

It occurs when localized attack at and adjacent to grain boundaries with relatively little corrosion of the grain takes place by the impurities at the grain boundaries [7, 8] (enrichment or depletion). The example of this type is austenitic stainless steel (sensitization) and heat affected zones of its wealds (HAZ) where the presence of carbon impurities (0.06 – 0.08%) at the grain boundaries of Cr (10%) leads to the formation of $Cr_{23}C_6$.

1.4.2.2 Dealloying.

Dealloying is characterized by preferential dissolution of one component of one alloy, typically leaching of a weak pseudo-morph of the original item. This form of attack is observed most often in gray cast iron (Graphitic corrosion) and in yellow brasses (Dezincification).

(I) Graphitic corrosion.

Graphitic corrosion may occur on the outside of cast iron pipe in corrosive soils [7, 8] and may be localized because of the difference in soil chemistry. It tends to be more general in distribution when cast iron pipe is attacked internally by aggressive water.

(II) Dezincification.

It occurs in yellow brasses where the zinc rich phase is dissolved and leaves a weak porous deposit of the copper rich phase which has a distinct reddish color [7]. It is called "layer type" when it is general in distribution and "plug type" when it is localized.

1.4.3 Corrosion identified through microscopic examinations.

1.4.3.1 Cracking.

There are two major types of cracking corrosion, which they are corrosion fatigue and environmental cracking.

(I) Corrosion fatigue.

It occurs due to the synergistic effects of repeated stress combined with corrosion [7].

(II) Environmental cracking.

It is a spontaneous brittle fracture of a susceptible material under tensile stress in a specific environment over a period of time. The environmental cracking is classified to stress corrosion cracking (SCC) [7] hydrogen assisted cracking (HAC) [7, 9] and liquid metal embrittlement (LME) [9].

1.4.3.2 High temperature corrosion.

This type of corrosion may be a surface phenomena or an internal effect within the structure of the metal or alloy [9]. The surface phenomena include oxidation or sulphidation, with an accumulation of metallic corrosion products and dissolution as by halogen attack or molten salt effect. Internal effects are also encountered due to reaction within the matrix with environmental species, which have diffused into the metal structure.

1.4.3.3 Biological corrosion. [5]

Corrosion of a metal can be caused by the metabolic activity of microorganisms either directly or indirectly. There are two types of microorganisms associated with this type of corrosion, which are aerobic and anaerobic. Aerobic types grow in an atmosphere contains oxygen, while anaerobic species grow in an environment devoid of atmospheric oxygen. The activity of these organisms may cause corrosion by:

(a) Producing a corrosive environment.
(b) Altering the resistance of the surface film.
(c) Having an effect on the rate of anodic or cathodic reactions.
(d) Creating electrolytic concentration cells on the metal surface.
(e) Altering the environmental composition.

As example, sulphate reducing bacteria (anaerobic) easily reduces inorganic sulfates to sulfides such as calcium sulfide or hydrogen sulfide. When these compounds come into contact with iron (such as underground iron pipes), conversion of the iron to iron sulfide occurs. Since these bacteria thrive under such conditions, the reaction will continue until the pipe fails. The damage can be reduced by chlorination or the addition of certain bactericides.

1.5 Corrosion monitoring techniques.

1.5.1 Non-electrochemical techniques.

1.5.1.1 Thermometric method.

A simple, rapid and limited method for comparing the inhibition efficiency of different additional agents [10]. It originally developed for aluminum and its alloys. According to this test, a piece of the metal of specified area is dropped into a definite volume of a corrosive solution. The variation of the temperature of the system is followed as a function of time. After an initial period of almost constant temperature, it raises quickly to attain a maximum value, which approaches in some cases the boiling point of the solution. A reaction number, R.N., was defined by Mylius as:

$$\text{R.N.} = \frac{T_m - T_i}{t} \qquad \text{K/min.} \qquad (1.9)$$

where: T_m = maximum temperature in K.
T_i = initial temperature in K.
t = time in minutes from the start of the experimental to attain T_m.

The reaction number is proportional to the rate of the corrosion of the metal. The extent of corrosion inhibition by a certain concentration of a particular additive is evaluated from the percentage reduction in the reaction number.

$$\%\ \text{Reduction in R.N.} = \frac{(\text{R.N})_{free} - (\text{R.N})_{add}}{(\text{R.N})_{free}} \times 100 \qquad (1.10)$$

where, $(R.N.)_{free}$ = R.N. in the corrosive medium.

$(R.N.)_{add.}$ = R.N. in the presence of additive.

1.5.1.2 Hydrogen evolution method.

Reactions in which gases are given of or taken up can be monitored by studying the change of gas amount over time. This method is also limited. The efficiency of a given inhibitor can be evaluated as the percentage reduction in reaction rate (K), so the percentage inhibition efficiency (%IE) can be calculated as follow:

$$\%\,IE = \frac{K_{free} - K_{add}}{K_{free}} x100 \qquad (1.11)$$

where: K_{free} = specific reaction rate in the corrosive medium.

$K_{add.}$ = specific reaction rate in the inhibited solutions.

and specific reaction rate constants (K) are calculated from the relation, V = K.t, where, (V) is the volume of hydrogen evaluated in cm^3 and (t) is the time in minutes.

1.5.1.3 Loss in mass method.

Loss in mass measurements are comprehensive testes for laboratory and field [11-14]. They are useful for metals or alloys, which are not subjected to special types of attack and form, which the products of corrosion are easily removed.

To determine the inhibition efficiency of certain inhibitor using these measurements, the metal sample should be polished, degreased, weighed and then immersed in the corrosive medium with and without inhibitor for certain time intervals at fixed temperature. The weight losses are determined after removing corrosion products and then thoroughly wash the specimens by distilled water dry and weigh.

The efficiency of inhibition is calculated from the mass loss values using the following equation:

$$\%\,IE = \frac{M_{free} - M_{add}}{M_{free}} x100 \qquad (1.12)$$

where, M_{free} = mass loss in the corrosive medium in mg cm^{-2}.

$M_{add.}$ = mass loss in the inhibited solutions in mg cm^{-2}.

Also, the corrosion rate is determined by the relationship:

$$C.R._{(mmpy)} = \frac{\text{wt. loss (mg)} \times 87.6}{\text{area (cm}^{-2}) \times \text{time (hrs)} \times d\ (\text{gm.cm}^{-3})} \times 100 \qquad (1.13)$$

1.5.1.4 Electrical resistance method.

This method involves the measurements of the change in the resistance of corroded metal by the equation: [11-13]

$$R_{metal} = \frac{\rho \times L}{A} \qquad (1.14)$$

where, R_{metal} = resistance of metal.

ρ = specific resistance.

A = area of cross section.

On corrosion, the area of specimen (A) is decreased. Hence the resistance (R) is increased. This means that the change in R value is correlated to corrosion rate (Kelvin or Wheatstone bridge).

1.5.2 Electrochemical techniques.

1.5.2.1 Open circuit potential method.

This method is used to measure the steady state potential (E_{ocp}), of the metal or alloy in the absence and in the presence of additives [15]. In this method, the potential of the corroding material is measured against a reference electrode at different time intervals until a steady state is reached. The steady state potential represents an equilibrium state at which ($I_{ox.}$) is equal (i_{red}).

1.5.2.2 Potentiodynamic polarization method.

(I) Tafel plots.

In this method, corrosion current can be determined from polarization curves by intercept method based on anodic and / or cathodic Tafel curves [16]. The corrosion rate of the system involves the measurements of potential of the working electrode for various applied current densities.

The relation between (E) and log (i) gives polarization diagram (Tafel plot). The intercept of anodic and cathodic Tafel lines provides the corrosion current and Tafel slopes give anodic (b_a) and cathodic (b_c) Tafel constants.

(II) Linear polarization method.

This technique is an accepted method of monitoring corrosion rates[17-20]. For a corroding metal, the polarization resistance (R_p), at small applied range of potential (5-20 mV) is related to the corrosion current density ($i_{corr.}$) by this equation:

$$i_{corr} = \frac{b_a.b_c}{2.3(b_a + b_c)} x \frac{1}{R_p} = \frac{B}{R_p} \qquad (1.15)$$

where, (b_a) and (b_c) are anodic and cathodic Tafel constants respectively, (R_p) is the polarization resistance and B equal the factor $\frac{b_a.b_c}{2.3(b_a + b_c)}$.

A controlled potential scan is applied over a small range, typically ±25mV with respect to E_{corr}. At a scan rate of 0.1 mV/sec, the resulting current is plotted against the potential. The slope of this linear potential-current plot at $E_{corr.}$ is identical with the polarization resistance which used together with the measured Tafel constants to determine the rate of corrosion.

The percentage inhibition efficiency (%IE) can be expressed as:

$$\% IE = \frac{i_{free} - i_{add}}{i_{free}} x100 \qquad (1.16)$$

where: i_{free} : corrosion current in corrosive medium.

i_{add} : corrosion current in presence of additive.

(III) Impedance method.

In recent years, the impedance technique has been widely used for measuring the corrosion rates of metals [21, 22]. The main advantage of this method is the complete elimination of the solution resistance. The equivalent circuit of a corroding metal which has both anodic and cathodic reactions under activation controlled may be represented as a parallel combination of charge transfer resistance (R_t), double layer capacitance (C_{dl}) and the solution resistance (R_s) in series.

From (R_t) value, the i_{corr} is obtained from the relationship:

$$i_{corr} = \frac{b_a.b_c}{2.303(b_a + b_c)R_t} \qquad (1.17)$$

An alternating voltage of 10-20 mV is applied, the resulting current and the phase angle (θ) is measured for various frequencies where, the impedance [Z = voltage/a.c] is resolved to a real part [$z' = z \cos(\theta)$] and imaginary part [$z'' = z \sin(\theta)$]. Plots of z' against z'' is a semicircle which cuts the real axis at high frequency corresponds to (R_s) and at low frequencies corresponds to ($R_s + R_t$) and the difference between the two values gives (R_t).

1.5.3 Surface examination techniques. [23, 24]

1.5.3.1 Scanning electron microscopy (SEM).

SEM is used for examination and analysis of the microstructured surface. It gives resolution of about (25A). It is useful for a quantitative identification of phases especially, for evaluation of microstructures geometry by image analysis.

Corrosion is studied with scanning electron microscopy to characterize the type of corrosion and kinetic of the processes. Degradation of microstructures during the morphological changes such as grain growth, particle coarsening and recrystallization are also investigated using (SEM).

The combination of x-ray, mapping and (SEM) is used to quantify the fractured areas in the ductile and brittle phases, the depth of dimples, and the size of the process zone in front of the crack and the mode of crack propagation to establish a quantitative model for fracture of the material.

1.5.3.2 Optical microscopy.

It is the most important tool for microstructure studies. Identification of unknown constituents may be aided by observation of their hardness relative to the matrix, by their natural color, by their response to polarized light and by their response to selective etchants. These observations are compared to known details about the physical metallurgy of the examined material. The basic components of the optical microscope are illumination system, condenser, light filter, objective lends and eye piece. Three types of illumination are used which they are:

- Bright field for the observations of microstructure.
- Oblique for the three dimensional appearance.
- Dark field for strong image contrast.

1.5.3.3 X-ray analysis.

It is used to study the crystal perfection, crystal structure, and dimension of phase diagrams, order-disorder transformation and chemical composition. Quantitative analysis is also possible because the intensities of the diffraction lines due to one constituent of a mixture depend on the proportion of that constituent in the specimen.

1.5.3.4 Auger electron spectroscopy (AES).

AES together with x-ray photoelectron spectroscopy (XPE) are the two major surface analysis techniques. (XPS) is more sensitive and gives more useful chemical informations, while, AES has the advantages of greater speed and the potential of high speed resolution. The idea of the two techniques depends on the ejection of electron from an inner shell, where the energy released appears either as an x-ray photon or transferred to another electron, which is ejected, from the atom with energy. The basic components of an (AES) are electron gun, electron spectrometer and electron detector.

1.5.3.5 X-ray photoelectron spectroscopy (XPS).

It has wide applications in the case of polymers, organics, biological specimens, fibers films, powders and particles. In this technique the specimen is excited by the excitation source and its subsequent response in the form of an emission of some species is observed by some types of microscopy.

1.6 Metallurgy and corrosion types of stainless steels.

Stainless steels (SS) are iron alloys containing a minimum of approximately 11% chromium, which prevents the formation of rust in the atmosphere [25]. They have been produced by basic electric arc process, Argon-oxygen decarburization (AOD) and electron beam process. They have been classified into ferritic, martenistic, austenitic, duplex and precipitation hardened types.

Stainless steels samples resist corrosion by the formation of a very thin transparent passive surface film of chromium oxide [26]. A supply of oxygen and a minimum level of 11% Cr dissolved in the matrix materials are necessary to maintain the surface film, which is self-heeling in air at room temperature. If

the film is not repaired after damage, the corrosion of stainless steels (SS) will be very rapid in most environments.

The content of Cr and Mo is very important [27]. Mo additions for good corrosion resistance and relative freedom from crevice corrosion in low velocity seawater depend on the level of Cr in the steel. Austenitic steels with 20-22% Cr require 6% Mo where ferritic steels with 25-28% Cr require 3% Mo. This Cr/Mo content, together with the influence of nitrogen content, has lead to the increased of the so-called pitting indices. The pitting resistance equivalent number (PREN) is obtained by:

$$PREN = \%Cr + 3.3.\ \%Mo + 16.\ \%N \qquad (1.18)$$

Stainless steels (SS) are used as construction materials for corrosion resistant equipments in most of the major industries, particularly in the nuclear, petroleum, power, food production, medical, chemical and electrochemical industries.

Stainless steels suffer from many types of corrosion, [25-30] such as general corrosion, pitting and crevice corrosion, intergranular corrosion (IGC), galvanic corrosion, stress corrosion cracking, hydrogen embrittlement, selective leaching and erosion corrosion.

1.6.1 General corrosion.

Stainless steels (SS) form a passive film and the resistance to various media depends on the base metal composition [30]. Types of stainless steels (SS) which have high level of Ni + Cr or Cr + Mo + Ni can exhibit higher corrosion resistance in reducing atmosphere. On the other hand, in oxidizing environmements, Stainless steels composition required for best corrosion resistance should contain high levels of Cr or Cr + Mo.

1.6.2 Pitting and crevice corrosion.

The higher Cr and Mo content are improving resistance in Cl^- environments. The other elements such as Ni, Cu and N also influence pitting corrosion resistance. Since Cr and Mo are ferrite forms, high levels of them provide ferritic phase, which exhibits corrosion resistance in variety of organic acids.

1.6.3 Intergranular corrosion (IGC).

To avoid grain boundary corrosion, the carbon level is reduced to 0.03% (low carbon grade). Ti and Nb are added as stabilizers and annealing heat treatment is done to redefuse the Cr back into the depleted areas [26]. As general, it is impossible to provide sufficiently low carbon to produce an unstabilized ferritic stainless steel resistance to (IGC) in the welded condition. There is only exception at 28% or higher Cr levels under 0.005% of carbon.

1.6.4 Galvanic corrosion.

The two metal corrosion may exist between (SS) and other materials immersed in a conductive and corrosive solution [27]. Stainless steels in passive condition are closely grouped. There are no substantial differences for austenitic, ferritic and duplex stainless steel in this respect.

1.6.5 Stress corrosion cracking (SCC).

For (SS) the specific corrosive medium is chloride. The most common solution to (SCC) of type 304 or 316 is to move to higher Ni level alloys. The ferritic (SS) with little or no Ni eliminates the (SCC) [28].

1.6.6 Hydrogen embrittlement.

It is a possible cause of damage in ferritic and also duplex stainless steels because of their high ferrite content [28]. Austenitic stainless steels are much susceptible and do not present a problem under most normal conditions.

1.6.7 Erosion corrosion.

Also, it is uncommon in different types of stainless steel [30]. It is not accelerated by seawater even in velocities reach to 8.2 m/sec.

1.7 Inhibition of stainless steel corrosion in aqueous solutions.

Inhibitors are chemicals that react with a metallic surface or the environment to give the surface a certain level of protection [31]. Inhibitors have been classified differently by various authors but the most popular classification regroup corrosion inhibitors as passivating, cathodic, organic, precipitation and volatile corrosion inhibitors. Inhibitors often work by adsorbing themselves on the metallic surface protecting the metallic surface by forming a film and slowing corrosion process by either increasing the anodic or cathodic

polarization, reducing the diffusion of ions to the metallic surface and/or increasing the electrical resistance of the metallic surface. The choice of a definite inhibitor depends on some considerations such as its cost, toxicity, availability and environmental friendliness.

Even though the stainless steel has good resistance to uniform corrosion, there are evidences where the stainless steels are attacked by localized corrosion in the working environment [32].

Pitting corrosion behavior of various stainless steels in chloride solution has been extensively studied by number of authors [33, 34]. Once pits are initiated they may continue to grow by a self-sustaining mechanism [7]. Pit initiation in perfect surface will be a result of certain interactions between discrete species in the environment and the passive surface. One among the species is chloride ion. The kinetic theory explains the breakdown of the passivity in terms of competitive adsorption between chloride ions and oxygen. The thermodynamic theory considers the pitting potential as that potential at which the chloride ion is in equilibrium with the oxide.

There are many references available in literatures for initiation of pitting with structure heterogeneity at the surface [35-37]. Many authors have studied the effect of MnS inclusion in stainless steels on initiation of pitting [38-41]. Thermodynamic instability of the sulphides leads to a dissolution tendency. Pitting attack has been associated with the presence of nonmetallic inclusions such as (Fe, Mn)S in corrosion medium [42, 43]. On the other hand few authors have studied the effect of sulphur species on the localized corrosion of stainless steel in chloride ions [44].

Henthorne, [45] has shown that the chromium content of the sulphides inclusions increases, when the total Mn content of the high sulphur martensitic stainless steel drops below 0.5%. When the Mn content of stainless steels drops below 0.4% the pitting potentials are shifted in the noble direction in chloride solution [46]. When there is an increase in the Mn content, there is a decrease in the pitting resistance in chloride solution [47].

The effects of Cl^- ion concentration and temperature on pitting potiantial of 316LSS were studied [48]. It was indicated that at higher temperatures, the

protective efficiency of the passive film decreases and at higher chloride ion concentration the pitting potential shifts towards the active value.

Harvath and Uhlig, [49] have shown that Cr and Ni, increase the pitting resistance. Mo an alloying element of stainless steel increases the pitting resistance [50-52]. The addition of Mo to nitrogen containing austenitic stainless steel improves their resistance to sensitization by retarding the precipitation of chromium carbides and by improving the passivation characteristic of the stainless steel [53].

The effect of chlorine addition to chloride on pitting of 304LSS has been studied [54]. The addition of chlorine shifts the corrosion potential, the break down potential and passivation potential of the alloy in the noble direction.

The difference in chemical composition, surface conditions, microstructure, mechanical stresses and thermal cycles in the weldement of stainless steels make the corrosion behavior of the weldement different from that of the parent alloy [55, 56]. Localized weld corrosion occurs if the weld metal contains high silicon and manganese. Weld metal with low Si (< 0.15%) has higher corrosion resistance than high Si (> 0.25%) weld metal. [57] Alloying elements are added to the coated electrodes as a means of modifying or controlling the chemistry of the weld metal deposit. Shlaby, [58] found failure of austenitic stainless steel welds due to pitting and crevice corrosion. Caul, [59] proved that welding can induce carbide precipitation, known as sensitization, particularly in the heat affected zone. He explained that high alloy fully austenitic stainless steel with low carbon (0.03%) can be welded without any loss of corrosion resistance at weld and heat affected zone (HAZ).

Studies of pitting resistance of series of welded Fe-Cr-Ni alloys containing various amount of Mo have shown that the pitting potentials on the metal are significantly more active than the corresponding values of the parent metal [60]. This effect was associated preferential pitting in Mo depleted austenite in the vicinity of delta ferrite precipitation during welding. The susceptibility of 316L weldement toward pitting and intergranular corrosion has been studied by Pujar etal. [61] Sridhar et al [62] have studied the effect of welding heat input and

summarized that higher heat input is beneficial for pitting corrosion resistance while welding of duplex stainless steel.

Pitting corrosion of stainless steel weldement occurred preferentially in the ferrite along the austenite-ferrite boundaries. The presence of delta ferrite within the microstructure of austenitic stainless steel weld joint was reported. [63] It was found that there was adulterous effect under conditions of high heat input during metal arc welding. Krishnan etal, [64] have studied the effect of ferrite content in the austenitic stainless steel welds on corrosion. The results showed that the presence of ferrite increases the corrosion rates in chloride.

Different surface-sensitive techniques were used to investigate localized corrosion of AISI 304 and 316 stainless steels in environments containing thiosulfate, chlorides, and sulfates. Pitting was induced in the laboratory using a scratch technique and electrochemical polarization [65]. Diameter of the pits was < 0.2 mm. Morphology of the pits and composition of corrosion products in the pits were studied. The surface pits were investigated directly after the electrochemical tests, on cross sections and on replicas. The surface-sensitive techniques used provided consistent results with valuable complementary information. Corrosion products in the pits contain high amounts of Cr and S as sulfides and sulfates. The pit deposit in the Mo-containing stainless steel contained additional a high amount of Mo. Indications of a thin chloride-rich layer next to the parent metal were found.

The influence of incident monochromatic UV light on the susceptibility of types 304 and 316 stainless steels to pitting corrosion in chloride-containing solutions is described [66]. Illumination of the immersed surfaces, in neutral and acidic solutions, give rise to an enhanced resistance to the onset of pitting corrosion that persisted for 220 h after the irradiation had been removed. This was evident from an increase in the breakdown potential, longer induction periods, and notable change is the current noise at constant potentials for specimens polarized under illumination. The degree of inhibition to pitting attack depended on the photon energy, the illumination period and the nature of the passive film. Higher breakdown potentials and longer induction periods

specimens previously kept 2, 24 and 120 h in NaCl solutions in order to assess the influence of pH on pitting corrosion susceptibility (with polarization tests) and the protective power of the passive film (with electrode impedance measurements). Corrosion films formed on free corroded specimens were characterized with XPS analysis. It was found that the corrosion current density (i_{corr}), corresponding to 316L steel's general corrosion as well as the passivity domain (Pd) are pH dependent in the whole exposure time range. The values of i_{corr} show a strong decrease with increasing pH, whereas Pd shows a U-shaped curve whose minimum value ranges between pH 4 and 8; higher values of the passivity domain have been ascribed to the presence of wet oxygen and of Mo^{VI} species which seem to increase the film electron resistance. For the shortest exposure time (2h) E_p value remains unchanged in a wide pH range (from 2 to 10) and increases only in highly alkali solutions pH 12 owing to the strong decrease of Cl^- amount in corrosion films formed in alkali environment. For the longest exposure time (120 h) E_p versus pH shows U-shaped curve with the lowest value in the pH range between 4 and 6. The effect of pH on critical pitting, found for long exposure times only, could be explained with prevailing formation in the passive layer of dry corrosion products containing Cl^-.

The pitting behavior of a range of iron-chromium thin film alloys, which are sulfide-free, has been studied by electrochemical methods coupled with in situ optical microscopy [70]. In 0.5M HCl, iron-chromium alloys with>~16 atom % chromium do not pit at any potential, whereas alloys with<~16 atom % chromium pit at approximately +500 mV standard calomel electrode. The sharp transition is believed to be associated with the existence of a critical size of iron cluster, which act as pit nucleation sites. This is modeled by the achievement of a high density percolation condition for iron in the body centered cubic alloy. The pits propagate under remnants of the passive film as two dimensional disks, with current densities up to 80 Acm^{-2} and simultaneous hydrogen evolution.

Potentiodynamic polarization curves were measured for types 304 (UNS S30400), 316L (UNS S31603), and 904L (UNS N08904) stainless steels (SS) in 1M sodium chloride solutions with various thiosulfate additions at temperatures from 20 to 90°C [71]. A minimum concentration of thiosulfate was required for

activation of pitting corrosion in each alloy, and this critical value was shown to increase with increasing molybdenum content and to decrease with increasing temperature. Above the critical thiosulfate concentration for type 904LSS, stable pitting occurred at temperatures up to 30°C below the chloride only critical pitting temperature. Also, polarization data at high thiosulfate levels exhibited an anodic peak thought to represent the oxidation of elemental sulfur, produced by prior reduction of thiosulfate at potentials < -450 mV vs. Ag-AgCl electrode.

Data from potentiodynamic polarization curves, current-time measurements and scanning reference electrode technique indicated that ultraviolet illumination of stainless steel 304 has a significant effect on corrosion in sodium chloride solution [72]. Either before electrochemical corrosion testing or during passivation at -100 mV (SCE), UV illumination was found to improve the passive film formed on a SS-304 surface or it inhibits pit growth. The pitting potential E_{pit} shifts positive if pH increases, under illumination. Current–time measurements reveal an increase in breakdown potential, longer induction periods, and notable changes in the curves at constant potential, for SS-304 electrodes illuminated either before electrochemical testing or during passivation.

The pitting corrosion of stainless steel was studied in 0.1M KCl in mixed solvents of water with methanol, isopropanol, 2-ethoxyethanol, ethylene glycol and acetonitrile solutions with various compositions (from 0.0 to 80 % volume of the organic solvent component) [73]. The results obtained from the potentiodynamic and potentiostatic measurements show that the pitting corrosion is inhibited by the organic components in the medium. The percentage inhibition was found to increase with increasing the concentration of the organic solvent in the medium and reached about 80% for some solutions. It is suggested that the organic solvents inhibited the pitting corrosion of stainless steel by increasing the viscosity of the medium, which leads to a decrease in the diffusivity coefficient for the diffusion of the corrosion products of the stainless steel out of the pit.

The Mylius technique works well for many exothermic reactions in acid/metal systems in immersed conditions [74]. In this paper the extent of corrosion of stainless steel exposed over mixed vapors of HCl and HNO_3 has been evaluated using the technique. It was found necessary to fix some experimental variables such as initial temperature and volume of acid solution to obtain uniform results. The maximum rise in temperature as well as the maximum corrosion was found with the vapors released by 2HCl : $3HNO_3$. The rate of attack increased with increasing acid concentration. It is possible to inhibit corrosion in the vapor phase by adding hexamine into the vapor-producing acid mixture.

A series of compounds having the N-acylamino acid or related structures were investigated as potential inhibitors of localized corrosion of AISI 304L stainless steel [75]. The effect of these compounds on the breakdown potential was measured using the linear current scan method. Interaction of the inhibitors with the electrode surface was studied using capacitance measurements and correlated with solution surface tension measurements. Successful inhibitors interact strongly with the AISI 304L surface, but the inhibition effect appears to involve more than just adsorption of the inhibitor. Evidence is presented for the formation of a hemimicellar inhibitor layer, which could exclude Cl^- ions from the surface or provide surface pH buffering. Formation of such layer is sensitive to the structure of the compound.

Lemaitre and Beranger, [76] studied the role of chromate and silicate ions as corrosion inhibitors of steel and stainless steel in neutral chloride medium, due to thermal fatigue, stress corrosion cracking or pitting. The inhibitive species act in the initiation of cracks. The efficiency of inhibitors was characterized by a critical value depending on the chloride content in the medium. The inhibition diagrams showed two mechanisms, which they are, the competitive adsorption of species, which contrast the passive layer and the diffusion through the passive scale.

The effect of C replacement with N in 15% Cr steel on corrosion behavior and mechanical properties was studied [77]. Nitrogen increased corrosion

resistance in H_2SO_4 and HCl solutions. The pitting corrosion potential was correlated with a parameter calculated from Cr, Mo and N contents. N decreased quenching hardness because nitride depleted interstitial atoms, which were essential for solid solution hardening. Tempering hardness was increased because nitride growth was slow.

Parazak et. al. [78], investigated the critical concentration chlorides for stainless steel pitting corrosion of the type Cr18Ni12Mo3Ti. A formula was deduced for the calculation of $[Cl]_{Cr}$ from the chemical composition of the working aqueous medium. The maximum allowed level of contamination of the medium and steel surface by chlorides were discussed for the condition found in some nuclear power plant system.

Lo Ping Ho et. al. [79], studied the effect of inhibitor (TDA) on corrosion of 12Kh18N10T and 20Kh25N20S2 stainless steels in solutions of 2% HCl (1) and 20 % H_2SO_4 + 40 g/L $NaNO_3$ (2), using electro-capillarity measurements. The type of surface activity of the above substances was studied. (TDA) behaves as a surfactant of molecular type with weakly expressed cationic properties. The corrosion rate was determined by the weight loss of the samples. The mechanism of the protective action of (TDA) inhibitor is the same in different solutions and does not depend on the chemical composition of the steel.

The effect of some organic additives on pitting corrosion of type 304SS in H_2SO_4 solution containing Cl^- ions has been studied [80]. From the results, the effects of the additives have been classified into three groups: the first group comprises the compounds, which inhibit both the active dissolution and pitting corrosion of the steel. The second group is characterized by retarding the active dissolution of the stainless steel, but catalyzing the pitting attack. The third group enhances both the dissolution and the pitting potentials.

The influence of calcium phosphate and seruim on the corrosion resistance of 316L stainless steel in 0.9% NaCl solution was investigated [81]. Both substances are responsible for an increase in the pitting corrosion resistance. Calcium phosphate accelerated the rate of film formation, enhanced the release of Fe and Ni and retarded that Cr from a corroding surface. Proteins

induced the incorporation of P and Ca in corrosion products. These effects appear to replicate the accumulation of the same elements observed on stainless steels corroded in vivo.

Olof et. al. [82], studied the corrosion properties of Ni alloys and stainless steel in acid chloride environments. The properties of amine corrosion inhibitors were also investigated. The effect of amines on the corrosion rate was studied in laboratory environment and in a depolarizer column for a cumene process.

Sanad et. al. [83], have been investigated the inhibitory effect of KI on the corrosion of different types of stainless steel in HCl solutions. It was found that KI was an excellent inhibitor for stainless steel types 316, 430 and 440 (more than 95 % efficiency) and moderate for the type 304. The corrosion rates in 1M HCl and in the presence of KI fit the Arrhenius equation. The presence of KI lowers the activation energy and rate of corrosion. Polarization measurements indicated that KI acts as cathodic inhibitor at lower concentrations. Also the synergistic effect of KI on organic substance was studied.

Kumar et. al. [84], studied the inhibitor efficiencies of substituted N-2-benzothiazolyl-N, N′, N″-triaryl guanidine at different concentrations in relation to the corrosion of stainless steel 304 in H_3PO_4-Cl at 25C° using Potentiodynamic technique. The inhibitor efficiency increased with increasing inhibitor concentration ≤ 50 ppm. N-2[(4-Methyl) benzothiazolyl]-N,N′,N″-tri-O-Me-Ph guanidine was the most effective inhibitor followed by N-2 benzothiazolyl- N,N′,N″ triphenyl guanidine, N-2[(5-chloro) benzothiazolyl]-N,N′,N″-tri-M-chloro-Ph guanidine, N-2[(6-chloro) benzothiazolyl]-N,N′,N″-tri-P-chloro-Ph guanidine. The marked influence of the inhibition was observed in decreasing the critical c.d. and enlarging the passive region.

The corrosion inhibition effect of hexamine, quinoline and thiourea on different types of stainless steel in 1M HCl solution was examined [85]. Polarization curves indicate that these compounds act as mixed type inhibitors. It can be concluded that the charge transfer reactions, i.e., $Fe \rightarrow Fe^{2+} + 2e$ and also, $H^+ + e \rightarrow H$ are inhibited simultaneously and individually by organic absorption film at the metal/solution interface and consequently the corrosion rate of (SS) is reduced effectively in hydrochloric acid solution. The results obtained for the different types of SS show that hexamine and quinoline are

more effective for SS type 430 and 440. The inhibitor concentration at which efficiency was above 80% was 10^{-2}M and 0.15M hexamine for the two types 430 and 440 respectively. In presence of quinoline, the maximum efficiency was ~90% at concentration 10^{-1}M for both types of SS. Thiourea was an excellent inhibitor for 316 type as the maximum efficiency was ~86% at 10^{-4} M.

The pitting corrosion behavior of SUS304 stainless steel in HCl/C_2H_5OH and $NaCl/C_2H_5OH$ aqueous solutions was studied [86]. It was found that the pitting potential shifted to the high side with an increase in scanning rate. The pitting potential shifted to the low side with an increase in the concentration of HCl and NaCl. The pitting potential shifted to the high side in more concentrated solution of ethanol. It was concluded that ethanol ion served as a kind of the organic inhibitor of pitting corrosion.

Chen and Zhang [87] studied the synergistic inhibition effect of sodium lauryl sulfate and monoethanol amine on the initiation of pitting corrosion of stainless steel 1Cr18Ni19Ti in neutral NaCl solution. The corrosion inhibiting effect was studied using various methods such as impedance and IR spectra.

The corrosion inhibitive efficiencies of substituted dithiomalon- amides were determined at different concentrations for 304SS in H_3PO_4-HCl mixture at 25°C using Potentiostatic technique [88]. The percentage inhibition efficiencies have been found to increase with increasing concentrations of inhibitors. 1, 5-Di-p-methylphenyl-2, 4-dithiomalon~ amide was found to be the most effective inhibitor followed by: 1,5-di-p-methoxyphenyl-2,4-dithiomalonamide; 1,5-diphenyl-2,4-dithiomalon~amide; 1,5-di-p-chlorophenyl-2,4-dithiomalonamide. Marked influence of the inhibitors is observed in decreasing the critical current density and enlarging the passive range.

The corrosion of 304 austenitic and 430 ferritic stainless steels in H_2SO_4 solutions was investigated using the polarization resistance technique [89]. Different organic inhibitors were used which contain an allyl group (CH_2:CH_2-). The effect of acid and inhibitor concentrations, temperature and addition of chloride ion was studied. Acid concentration was varied between 2 and 12 M and the reaction rate was maximum at 6 M. The inhibition efficiencies of various compounds were dependant on the concentration and vary from one

alloy to another. For 304SS the efficiency lies between 40-100%. For 430SS some of these compounds behaved as a corrosion accelerator at certain concentrations and inhibitors at others. Chloride ions improved the inhibition efficiency with some exceptions. Various kinetic parameters were evaluated and are reported. In addition the reaction mechanism is briefly discussed.

Ismail et. al. [90], examined the inhibition effect of semicarbazide, thiosemicarbazide, 1, 5-diphenyl carbazide and sym- diphenyl carbazide one two different types of C-steel and 304 stainless steel in 10 % HCl solution by means of electrochemical polarization measurements. It has been found that thiosemicarbazide has a significant effect on the corrosion of the two types of C-steel (0.16 and 0.8C), and the protection efficiency more than 85%. Sym-diphenyl carbazide more effective for 304 stainless steel and the inhibition efficiency is approaching to 80%. Polarization measurements have indicated that these compounds act as mixed types inhibitors. Also, the effect of structural changes of these compounds on their inhibition has been studied.

La and Sm nitrates and chlorides were investigated as corrosion inhibitors for AISI 434 stainless steel in NaCl solutions at room temperature [91]. Electrochemical techniques allowed an evaluation of the degree of protection and cathodic nature of the inhibitors. SEM and energy dispersive spectrometry were used to analyze composition of the protective films formed after full immersion tests.

The corrosion behavior of two types of C-steel and 304 stainless steel in hydrochloric acid solutions alone and in the presence of semicarbazide, thiosemicarbazide, 1,5 diphenylcarbazide and sym-diphenyl carbazide was studied by weight loss measurement at different temperatures (303 to 343 K) [92]. Linear Arrhenius plots were obtained in the absence and presence of inhibitors. Results elucidate the effect of temperature and molecular structure on the inhibition efficiency. Thermodynamic parameters for adsorption of these compounds were calculated using the Temkin adsorption isotherm.

Zhan Guojin et. al. [93], have been tested the inhibition efficiencies of different concentrations of benzoimidozole compound (BMAT) on 316L stainless steel in 5% HCl by weight loss measurements. Adsorption of (BMAT) obeyed the Frumkin isotherm. The corrosion inhibition was considered to be chemisorption by studying the influence of temperature on 316L stainless steel. Testing of polarization curve showed that (BMAT) was mainly cathodic but mixed inhibitor.

Zhu Yifan, [94] investigated the corrosion resistance of stainless steel (AISI 316L, AISI 304) and carbon steel in acidic waste water (pH = 2.1, 30°C) containing phenol using potentiostatic polarization curves and weight losses of rotary specimens. The stainless steels have good corrosion resistance, but carbon steel (Model 20) has not. Formaldehyde in the acidic wastewater may inhibit corrosion of the stainless steels. Compared with the corrosion in the hydrochloric acid solution of the same pH, the inhibition was 70% complete.

Benzotriazole and 2-aminotriazol were studied as inhibitor of corrosion of 304SS in 1.0 M H_2SO_4 solution [95]. Weight loss, electrochemical polarization, SEM and AES techniques were employed. Experiments were carried out using 100, 200 and 400 ppm concentrations of the studied inhibitors at 20, 30 and 40°C. Tafel slopes have been measured by galvanostatic polarization and corrosion rates were computed using Stern-Geary equation. Inhibition efficiency increases with the increase in concentration of inhibitors and decreases with the increase in temperature. Both the inhibitors obey Langmuir adsorption isotherm. Benzotriazole is chemisorbed and 2-aminothiazole is physically adsorbed. Benzotriazole acts as a mixed inhibitors but anodic character is more predominant while 2-aminothiazole is cathodic in nature.

DL-methionine was investigated as inhibitor for corrosion of 304SS in 1.0 M H_2SO_4 solution [96]. The inhibition efficiency increases with the increase in concentration of the inhibitor and decreases with the increase of temperature. Crit. c.d. and passivation c.d. values decrease with increasing concentration of the inhibitor. It is physically adsorbed on the surface of steel and acts as a mixed inhibitor. Longmuir's adsorption isotherm fits the experimental data for the

studied compound. Adsorption of DL-methionine occurred through the nitrogen of the molecule. The inhibition imparts higher values of activation energy for the corrosion reaction.

Viorel et. al. [97], investigated the inhibitory effect of some surfactants on corrosion of stainless steel W. 4541 in an aqueous 0.5N HCl solution by the use of potentiostatic method. At lower voltage values the dissolution process was controlled by activation, while at the high overvoltages values, the dissolution process was controlled by diffusion. The corrosion inhibition was determined using three surfactants. The efficiency of the test corrosion surfactants decreased in the order: $H.T > C_{25}H_{46}NClH_2O > C_8H_{16}NCl$
where, the process of inhibition was attributed to the formation of adsorbed film on the metal that protected the metal against the corrosive agents.

Xiong et. al. [98], studied the mechanism of corrosion inhibition of $K_2Cr_2O_7$ on surface of 304 stainless steel. When 1% $K_2Cr_2O_7$ was added to 3.5% NaCl solution the maximum dissolution currents ($I_{max.}$) of 304SS was decreased. The minimum dissolution currents ($I_{min.}$) varied regularly with the applied potential. The curves of I_{max}-V and I_{min}-V shifted towards positive potential. The time for repassivation of the surface of 304SS was shortened.

The effects of sulfur-containing compounds on anodic processes on iron and stainless steels were studied using the electrochemical method [99]. In the low potential range KSCN can catalyze the anodic dissolution of iron in 0.5 mol/dm^3 H_2SO_4. The influence of KSCN decreases with increasing electrode potential. In corrosion catalysis process of KSCN, the desorption of KSCN increases with the anodic dissolution current of iron. The catalysis of KSCN on the anodic dissolution of austenitic SS is much stronger than on ferrite SS. KSCN has no influence on the reactivity process of iron in sulfuric acid, while the reactivation potential of ferrite SS is improved notably by KSCN.

2-Aminobenzene arsenic acid was investigated to control the corrosion of 304SSin 0.1M H_2SO_4 solution by using weight loss, polarization resistance, SEM, and Auger electron spectroscopy techniques [100]. Inhibition efficiency was

found to increase with increasing concentration of the inhibitor but decreases with increasing temperature. Various corrosion parameters like Tafel slopes, corrosion rate, heat of adsorption and activation energy were evaluated to understand the mechanism of inhibition. 2-Aminobenzene arsenic acid is physically adsorbed on the surface of 304 stainless steel and obeys Langmuir's adsorption isotherm equation.

The effect of benzotriazole ($C_6H_3N_5$) as a corrosion inhibitor for type 304 stainless steel in 2M H_2SO_4 was studied using weight loss experiments, anodic and cathodic potentiostatic measurements, atomic emission spectrometry, optical and SEM [101]. Benzotriazole acted as a corrosion inhibitor over the entire range of potentials studied, from -625 to +1250 mV with respect to a SCE, and did not promote selective alloy dissolution. The protective film was stable and adherent and obeyed the Langmuir isotherm, while values of the equilibrium adsorption constant suggested chemical adsorption. The maximum coverage obtained was 0.97 for stirred solutions and 1.0 for unstirred solutions, these values being associated with partial dissolution and lack of dissolution of inclusions respectively.

The effect of samarium on the corrosion behavior of different types of stainless steels in NaCl + Sm (III) solutions was studied by electrochemical methods [102]. The results allowed the evaluation of the efficiency of Sm (III) as a corrosion inhibitor by the kinetic parameters of the oxygen reduction reaction and the electrochemical behavior of steels. The behavior observed depends on the nature of the steel and the inhibition phenomena associated with a surface modification due to a hydroxy –samarium compound layers formed at the steel surface, as confirmed by EDS anal. Studies.

The early stage of pitting corrosion of 430 stainless steel in 0.5M NaCl solution containing 0.01, 0.05 and 0.1M Na_2SO_4 have been studied by an AC impedance method [103]. It was found that the Warburg impedance coefficient (σ), which was calculated from Nyquist plots, decreases with increasing Na_2SO_4 in the solution at a given potential in passive region. This is because that increasing SO_4^{-2} concentration in NaCl solution decreases the total number of

surface sites available for metastable pits. The change in E_m (the potential at which metastable pit or pits start to grow on the steel) is a function of SO_4^{-2} concentration in NaCl solution. The values of E_m in millvolts are linear with logarithm of SO_4^{-2} concentration of 0.5M NaCl solution, following the equation:

$$E_m = 59 \log (SO_4^{-2}) - 114 \qquad (1.19)$$

This fact suggested that, increasing SO_4^{-2} concentration in NaCl solution causes the shift of not only pitting potential but also E_m to more positive potentials.

Corrosion inhibition by methionine (MET), citrulline (CIT), alanine (AL), glycine (GLY) and hydroxyproline (HPR) with respect to the dissolution of tungsten stainless steels in hydrochloric acid solution was studied using potentiodynamic, Tafel extrapolation and polarization resistance methods [104]. Polarization curves indicated that the primary passivation potential (E_{pp}) and the transpassive region shift towards more positive potentials in presence of the studied amino acids, i.e. there is more passivation at wide potential range in the presence of amino acid inhibitors. The corrosion parameters are dependent on the percentage of tungsten in the alloy composition as well as the nature of the tested amino acids. The intermetallic compound Fe_3W_2 may form a galvanic cell with the matrix around the Fe_3W_2 phase within the matrix that is formed as a dispersed phase.

The effects of several oxoacid salts (sulfate, molybdate, phosphate, and nitrate) on pitting behavior of type 304SS (UNS S30400) were examined to characterize their performance in high temperature chloride solutions through measurement of pitting temperatures (T_p) and potentials (E_p) [105]. Measurement of E_p at a given temperature, as usually adopted, did not provide sufficient information to characterize oxoacid salts as pitting inhibitors because the unique potential dependency for the inhibitive action could be missed, as was the case for nitrate. In addition, whether pitting occurred on heating could not be predicted because pitting could not be inhibited as effectively at lower temperatures as at higher temperatures, as in the case of molybdate and phosphate. Temperature versus current density (CD) curves at given potentials were extended beyond 373 K using an autoclave system and were measured in addition to potential versus CD curves. The combined data provided extensive

information on the inhibitive action of each oxoacid salt. Sulfate seemed to work through adsorption, while molybdate and phosphate were incorporated into the passive film, which proceeded more extensively at higher temperatures. Nitrate had a critical potential to inhibit pitting below which it scarcely worked, although its role was not understood satisfactorily. This explained why nitrate did not shift E_p at 423K as extensively as at 298K, where the E_p in 0.5 M NaCl solution was as low as -70 mV versus a standard hydrogen electrode.

Pitting corrosion studies, [106] carried out on types of 304, 316 and 317 stainless steel containing nitrogen in a medium containing 0.5M NaCl and 0.5M H_2SO_4 indicated that the addition of nitrogen improved the pitting resistance more so, in the case of Mo-containing alloys. XPS analysis of the passive films indicated significant changes in the nature and component of the passive films with nitrogen content. The dissolution studies at the active potential indicated the segregation of N and Mo at the surface when analyzed by secondary ion mass spectrometer (SIMS). A mechanism by which N improves the passive film stability and pitting corrosion resistance was proposed. In the presence of N the growth of the stable pit is delayed as N stabilizes the repassivated film during initial stage of pit formation. N present at the pit site along with Cr and Mo forms of ammonium ion and other inhibiting compounds and this increase the pH of the solution inside the pits and stabilizes the passive film against further pit growth. This widens the passive range in which pitting is less probable and increases the resistance against pitting attack.

Santos et. al. [107], investigated the corrosion protection of carbon steel and stainless steel by polyaniline films. The potentiodynamic polarization curves were obtained for carbon steel and stainless steel in contact with 3% NaCl saturated with air in order to evaluate the capacity of polyaniline in the emeraldine oxidation state to protect the surface against corrosion processes. A high stability of polyaniline films was observed, with a gain of the corrosion potential around 270 mV more positive in the substrate covered with polyaniline than in the case without it. Corrosion of steel could be prevented using conducting polymers as a protective layer.

The corrosion behavior of ferritic type 430 and 444 stainless steels in oxalic acid solutions was investigated by measuring the corrosion weight loss, DC polarization and natural electrode potential (NEP) variations with time [108]. Elements dissolved in oxalic acid solution after weight loss test were analyzed by atomic absorption analysis and by ultraviolet absorption spectroscopy. The stability constants for the formation of Fe^{2+} oxalate and Cr^{3+} oxalate complexes were obtained, and the relation between the stability and corrosion behavior was also investigated from thermodynamic parameters. The atomic absorption analysis clarified that the amount of dissolved Chromium was the same as that corroded Cr, and hence Chromium seemed to be completely dissolved into the solution. The UV- visible absorption spectroscopic analysis revealed the formation of $[Fe (C_2O_4)_3]^{-2}$ and $[Cr (C_2O_4)_3]^{-3}$ in the solutions after corrosion weight loss test. The formation of these complexes was also estimated from the values of successive stability constants. Thermodynamic parameters for the formation of Fe^{2+} oxalate and Cr^{3+} oxalate were obtained from Vent's Hoff plot. The Gibbs free energy values for Fe^{2+} and Cr^{3+} oxalate became larger with increasing solution temperature.

The effect of Cr (VI) species in HNO_3 (concentrations 15-3 M) on the corrosion rate of stainless steel has been investigated [109]. The gaseous phase over the HNO_3 was carefully controlled using Ar, NO, NO_2 or N_2 purging. With Ar purging the corrosion rate increased when the Cr (VI) concentrations were above 0.05 M. there was evidence that the reduction of Cr (VI) leads to insoluble Cr reduction products on the surface of the steel. Sparging of nitric acid by NO and/or NO_2 caused the reduction of any Cr (VI) species present in the solution, to Cr (III) in a few minutes. However, with no Cr (VI) present, the effect of continuous purging with NO and/or NO_2 was to increase the steel corrosion rate when compared with Ar purged solutions, due to catalysis of nitrate reduction by the NO_x. The conversion of Cr (III) to Cr (VI) by nitric acid was shown to require high concentrations of nitric acid, high temperatures and low partial pressures of NO_2 over the liquid phase.

The effect of benzotriazole (BTAH) as a corrosion inhibitor for type 304 stainless steel in 2M H_2SO_4 water-ethanol (80:20) solutions was studied using

weight loss experiments, anodic and cathodic potentiostatic measurements, and analysis by SEM [110]. BTAH increases the corrosion rate at lower concentrations ($\leq 3.0X10^{-6}M$) but it provides complete inhibition when [BTAH] $\geq 1.5X10^{-4}M$. The catalytic effect was also observed from anodic potentiostatic curves for [BTAH] $\leq 10^{-6}M$ over the entire active potential range. A synergistic effect was observed in the presence of ethanol for higher BTAH concentrations. When the system was compared with those in aqueous media. BTAH acts as cathodic and anodic inhibitor over the entire range of potentials studied.

The adsorption behavior of piperdine (PD) as an inhibitor on passive film of stainless steel was studied by using quantum chemistry methods [111]. Three kinds of quantum chemistry methods, semiempirical SCF/PM3 (improved MNDO), ab initio SCF/STO-3G and SCF/6-31G were applied to clarify the origin of good inhibition performance of PD on passive films of stainless steel. According to the data of formation heat and adsorption energy of molecules with different possible confirmation, the chair style conformation of PD is stable. With OFeOFeO and OCrOCrO being succedaneums of one dimension oxide film, the optimized geometry and electron energy level of these molecules were calculated by ab initio SCT/STO-3G. On the basis of chemical reaction generalized perturbation theory, the interaction between PD and metal oxide was discussed. The results indicated that the adsorption of PD on passive film is a charge control reaction. The adsorption of PD can be described to N atom acting as electron donor to chelates with Fe and Cr atoms in oxide film. The obtained adsorption bond energy is in agreement with the single bond energy of normal Fe, Cr complexes including N atoms. Moreover, the adsorption orientation of PD on passive film was deduced preliminarily.

The corrosion behavior of several austenitic and ferritic stainless steels was studied in the KCl-NaCl-$BaCl_2$ melt (molar ratio 1:1:1) at 600°C in the absence and presence of 0.1M sodium salts with different oxy-anions, namely, Na_2CO_3, Na_2O_2, Na_2SO_3, Na_2SO_4, Na_3PO_4 and $Na_4P_2O_7$ [112]. The corrosion rate, determined from analysis of the melt by atomic absorption, was found to agree well with that determined from anodic polarization and decreased with increasing percentage Cr in the alloy. The presence of the oxy-anions decreased

the corrosion rate in the order: $P_2O_7^{4+} < PO_4^{3-} < SO_3^{2-} < SO_4^{2-} < O_2^{2-} < CO_3^{2-}$ which runs parallel to the order of increasing ability of O^{2-} ion donation and indicates that the inhibition process involves the formation of the passivating film on the surface. All stainless steels suffer a significant selective leaching of chromium and among all the oxy-anions tested; only CO_3^{2-} anions suppressed the dechromization in the KCl-NaCl-$BaCl_2$ melt significantly

The electrochemical behavior of 316 stainless steel in H_3PO_4-Cl^- solutions containing nitrate, dichromate, tungstate, and molybdate anions as inhibitors are presented and discussed using potentiodynamic and potentiostatic polarization techniques [113]. The results showed that most additives improve the corrosion resistance of the alloy. The additives retard both active and pitting attack to an extent depending on the type and concentration of the additive. Results were correlated with the beneficial action of the corresponding alloying elements.

The application of Auger Electron Spectroscopy (AES) to the study of the composition and thickness of the passive film formed on the surface of 316 stainless steel in H_3PO_4-Cl^- solutions containing nitrate, dichromate, molybdate and tungstate as inhibitors is discussed [114]. Data are presented which explain the effectiveness of the additives on the properties of the passive films of the alloy. It is concluded that much higher corrosion resistance of the alloy is observed in nitrate additives due to marked nitrogen enrichment underneath the passive film, which enhances the repassivation ability of this alloy. The results could also explain the effectiveness of the dichromate, molybdate and tungstate anions due to improved film repair conditions.

Park et. al. [115], studied the effect of bicarbonate ions (HCO_3^-) on pitting corrosion of type 316L stainless steel in aqueous 0.5 NaCl solution using potentiodynamic polarization, the abrading electron technique, Alternating current (AC) impedance combined with X-ray photoelectron spectroscopy (XPS) and scanning electron microscopy (SEM). Addition of HCO_3^- ions to NaCl solutions extended by passive potential region in width and at the same time raised the pitting potential in value on the potentiodynamic polarization curve. Potentiostatic current transients obtained from the moment just after

interrupting the abrading action showed the repassivation rate of propagating pits increased and that the pit growth rate decreased with increasing HCO_3^- ion concentration. Over the whole applied potential, the oxide film resistance was higher in the presence of HCO_3^- ions. The pit number density decreased with increasing HCO_3^- ion concentration. Moreover, addition of HCO_3^- ions to NaCl solutions retarded lateral pit growth, while promoting downward pit growth from the surface. The bare surface of the specimen repassivated preferentially along the pit mouth and walls compared to the pit bottom, as a result of formation of surface film with high content of protective mixed ferrous chromous carbonate that formed from preferential adsorption of HCO_3^- ions.

The influence of the organic sulfur-containing compounds on the corrosion of some ferrite and austenitic stainless steel types in sulfuric acid was studied [116]. The results showed that the anodic dissolution and self-corrosion of stainless steels were remarkably accelerated in solutions with a low amount of organic sulfur-containing compounds (0.02 mmol/dm^3). With an increase of the organic sulfur-containing compound concentration, more and more the organic sulfur-containing compound moles absorbed on the electrode surface and segregated the metal surface from the solution, which caused the decrease of the anodic dissolution and hydrogen evolution current of stainless steels. The anodic polarization behaviors of stainless steels were also changed with the various types of the organic sulfur-containing compounds and stainless steels.

The potentiodynamic anodic polarization behavior of AISI 304 stainless steel (SS) in 0.1 M NaCl containing various concentrations of SO_4^{2-}, SO_3^{2-}, S^{2-}, SCN^- or $S_2O_3^{2-}$ anions was studied [117]. In pure chloride solutions, the alloy exhibited pitting corrosion. The addition of low concentrations of the sulfur containing anions (except SO_4^{2-}) decreases the pitting potential. The sulfate anion appears to increase the pitting potential. The electrical charges associated with the pitting initiation and propagation processes were calculated when the steel was immersed under potentiostatic potential of +320 mV for 10 min in 0.1M NaCl without and with 10^{-2} M of the cited anions. The results indicated that SO_3^{2-}, S^{2-}, SCN^- and $S_2O_3^{2-}$ anions promote the chloride-pitting propagation

kinetics. The pitting potential of 304 SS decreases linearly with increasing chloride concentration while it was temperature independent in chloride and chloride containing sulfur anions in the range from 40 to 70°C. SEM observations indicated that open pit with 250μm in diameter produced on the steel in 0.1M NaCl under constant potential of +320 mV, while salt film formation inside open pits produced in the presence of sulfur containing anions with chloride. The pit morphology and its diameter depend on the type of sulfur containing anion present.

The effect of Rhodanine azosulpha drugs on the corrosion behavior of 304 stainless steel type in 1.0 M HCl solution as corrosive medium has been investigated using weight loss and potentiostatic polarization techniques [118]. Some corrosion parameters such as anodic and cathodic Tafel slope, corrosion potential, and corrosion current, exchange current densities, surface coverage and inhibition efficiency were calculated. The polarization measurements indicated that the inhibitors are of mixed type and inhibit corrosion by parallel adsorption on the surface of steel due to the presence of more than one active centre in the inhibitor molecule. The adsorption is obeyed Langmuir adsorption isotherm. The activation energy and thermodynamic parameters were calculated at different temperature.

The corrosion behavior of 304SS in 0.5M H_2SO_4 solution was studied using potentiodynamic and galvanostatic polarization techniques [119]. Three anodic peaks were observed in the Potentiodynamic anodic polarization curves before oxygen evolution. The first anodic peak due to the formation of Fe, Cr and Ni oxides. The second peak due to the formation of higher oxides of Fe and Cr and the last anodic peak due to the formation of Fe, Cr and Ni hydroxides. The inhibitive effect of 4-subistituted pyrazol 5-one toward the corrosion of 304SS in 0.5M H_2SO_4 was studied. The inhibition action of these compounds was assumed to occur via adsorption on the steel surface through the active centers contained in their structure. The mechanism of inhibition was interpreted on the basis of the inductive and mesomeric effects of the substituents. There is

a good agreement between the percentage inhibition efficiencies calculated from both techniques. The inhibition efficiencies increase with increasing the inhibitor concentrations.

The anticorrosive behavior of octadecylamine (ODA) films has been investigated via weight loss and electrochemical methods [120]. Tests were conducted on specimens of carbon steel, brass, and austenitic stainless steel in the presence and absence of amine films. Inhibitor efficiency values in excess of 94.5 % were obtained in this series of experiments. These results have been applied for the protection of boiler surfaces when out of service. For surfaces that were coated with ODA before lay up began, the optimum concentration of ODA for protection while out of surface was found to be 0.2 ppm.

The inhibitive effects of chromate and molybdate on pitting corrosion in stainless steel of the types 304 and 316 were studied in acidified chloride solution [121]. The results presented show that these known inhibitors affect both the nucleation of pitting and metastable pitting by reducing the numbers and sizes of these events. This makes attainment of stable pit growth more difficult.

The corrosion and electrochemical behavior of 316S11 stainless steel in acetic acid solutions typifying chemical process environments has been investigated [122]. Acetic acid concentrations tested were in the range 70- 90% and included addition of 1500 ppm Br^- and 200 ppm Na^+. Of key interest was the impact of Cl^- ions, representing an uncontrolled excursion in system chemistry. Corrosion potential-time and electro-chemical polarization measurements were made for the different environments at 90°C and the characteristics of the surface film formed at different stages of exposure analyzed using x-ray photo-electron spectroscopy (XPS). The most distinctive feature of the results was the step increase in potential with exposure time in the 70% acetic acid solution, in the absence of Cl^- ions, indicating a sharp transition from active corrosion to some degree of passivity. No such transition was observed in the 90% acetic acid solution. Addition of Cl^- to the 70 % acetic acid solution after the step in potential resulted in a decrease in potential once a

critical level of Cl^- had been exceeded. If the Cl^- were present on initial immersion, the potential stayed low and the steel remained active. XPS analysis suggested that local enrichment of Mo was important in initiating the passivation process but the precise details of the mechanism remain speculative.

The inhibiting effect of some aliphatic diamines (ethylen-diamine, 1,3 propane-diamine; 1,4 butane diamine; 1,8 octandiamine and 1,12 dodecane-diamine) and aromatic diamines (1,2 phenylene diamine; 1,3 phenylene diamine and 1,4 phenylene diamine) on the corrosion of irradiated and non-irradiated 304 stainless steel in 1M HCl at different temperatures was investigated [123]. On using two independent techniques, weight loss and Potentiodynamic polarization techniques it was found that, the values of inhibition efficiencies (%P) for aliphatic diamines obeyed the order (1,8 octane-diamine > 1,12 dodecane-diamine > 1,4 butane-diamine > 1,3 propane-diamine > ethylen-diamine) and for aromatic diamine the order was (1,3 phenylene diamine >1,4 phenylene diamine > 1,2 phenylene diamine). Also, thermodynamic parameters of activation (ΔH^*, ΔS^*, E_a^*) and adsorption ((ΔG^o_{ads}, ΔS^o_{ads}, Q) were calculated and discussed. From comparison it was concluded that by increasing the dose of (γ) radiation, the inhibition of the used diamine inhibitors was increased. All the given data obtained from polarization techniques suggested that, the above mentioned diamine compounds act as mixed type inhibitors. Also, E_{corr} values were shifted to less negative values by increasing the concentration of diamine compounds. Moreover, i_{corr} values of (γ) irradiated AISI 304 stainless steel were less than that for non-irradiated type which indicated that (γ) radiation retarded the corrosion rate.

1.8 Crown ethers as corrosion inhibitors.

Although alkali and alkaline metal cations play an important role both in chemistry and in biology, the coordination chemistry of alkali and alkaline metals was completely ignored by chemists. However, the coordination chemistry of alkali and alkaline cations has mainly developed by the synthesis of crowns by Pedersen [124, 125]. He reported the synthesis of over 50 cyclic

polyethers in which the size of the macro-cyclic rings, the number of ether oxygen, the number and the type of their constituent groups on the ring were varied widely. For example, the polyether ring contained from 9 to 60 atoms of which 3 to 20 were oxygen atoms. The structures of some crown ethers, their names and code designations are given in Fig. (1.1).

The discovery of the crown ethers was followed by the synthesis of macrocyclic polyethers containing three polyether strands joined by two-bridgehead nitrogen. These compounds have three-dimensional cavities, which can accommodate a metal ion of a suitable size and form an inclusion complex. Also, these ligands are called 2-cryptands [126], where 2, indicating the bicyclic ligand. The structures of some 2-cryptands, their names and code designations are given in Fig. (1.2). Also, 3 and 4-cryptands have been synthesized [127-134] and their typical structures are given in Fig. (1.3).

The crown ethers and their thia- and aza- derivatives have considerable interest in terms of their complexation properties in solution not only with alkali cations but also with other univalent and bivalent metal ions and substituted protonated amines [128, 129].

The most important factors that influence the selectivity and binding properties of macrocycles include arrangement of ligand binding sites [141], Fig. (1.4), type and charge of metals [131], type of donor atoms [132], number of donor atoms [133], substitution on the macrocyclic ring [132], and type of solvent [134, 135].

There are many different uses of crown ethers in analytical chemistry [136], corrosion chemistry [137], biological activity [138, 139], phase transfer catalysts [140, 141]. Moreover there are many applications of crown ethers in nuclear energy, electronics, electrochemical photosensitive materials, military and other uses have been investigated [142].

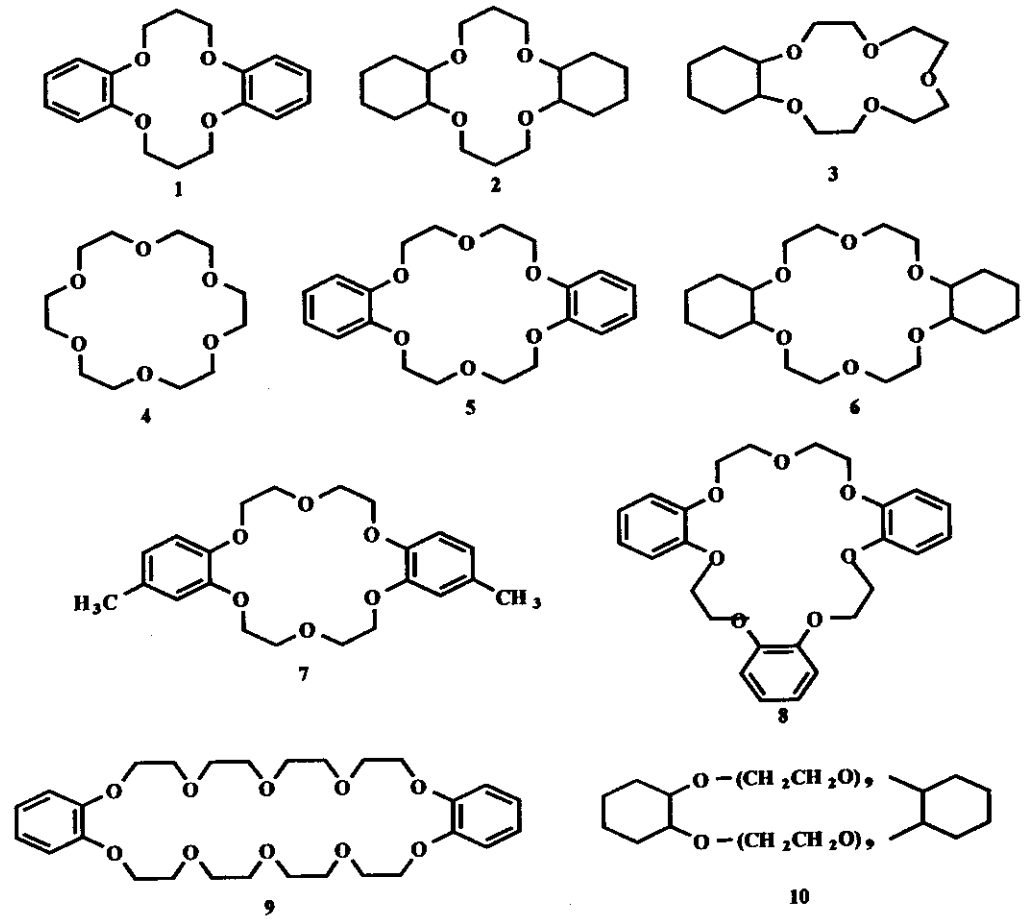

Fig. (1.1): Structural formula of some typical crown ethers. The trivial names and codes are listed below: -

(1)	Dibenzo-14-crown-4	DB14C4
(2)	Dicyclohexyl-14-crown-4	DC14C4
(3)	Cyclohexyl-15-crown-5	C15C5
(4)	18-crown-6	18C6
(5)	Dibenzo-18-crown-6	DB18C6
(6)	Dicyclohexyl-18-crown-6	DC18C6
(7)	4,4′-Dimethyldibenzo-18-crown-6	4,4′DMeDB18C6
(8)	Tribenzo-21-crown-7	TB21C7
(9)	Dibenzo-30-crown-10	DB30C10
(10)	Dicyclohexyl-60-crown-20	DC60C20

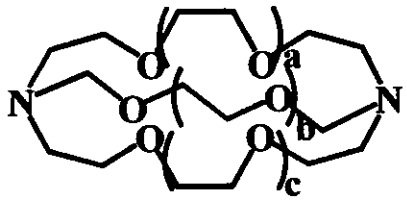

11-17

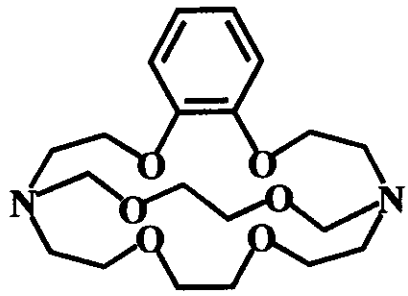

18

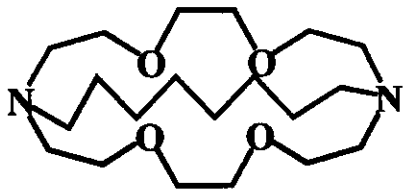

20

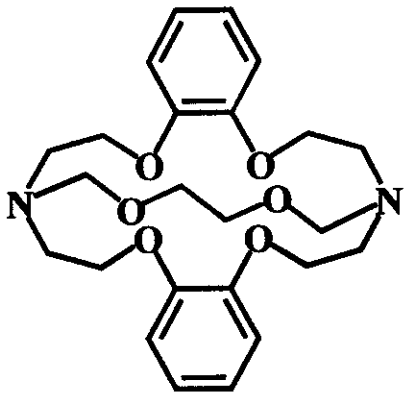

19

Fig. (1.2): Structural formula of some typical [2]-Cryptands.

(11)	a = b = c = 0	Cryptand 111	C111
(12)	a = b = 0, c = 1	Cryptand 211	C211
(13)	a = 0, b = c = 1	Cryptand 221	C221
(14)	a = b = c = 1	Cryptand 222	C222
(15)	a = b = 1, c = 2	Cryptand 322	C322
(16)	a = 1, b = c = 2	Cryptand 332	C332
(17)	a = b = c = 2	Cryptand 333	C333
(18)	_____	Monobenzo Cryptand 222	C222B
(19)	_____	Dibenzo Cryptand 222	C222DB
(20)	_____	_____	$C22C_s$

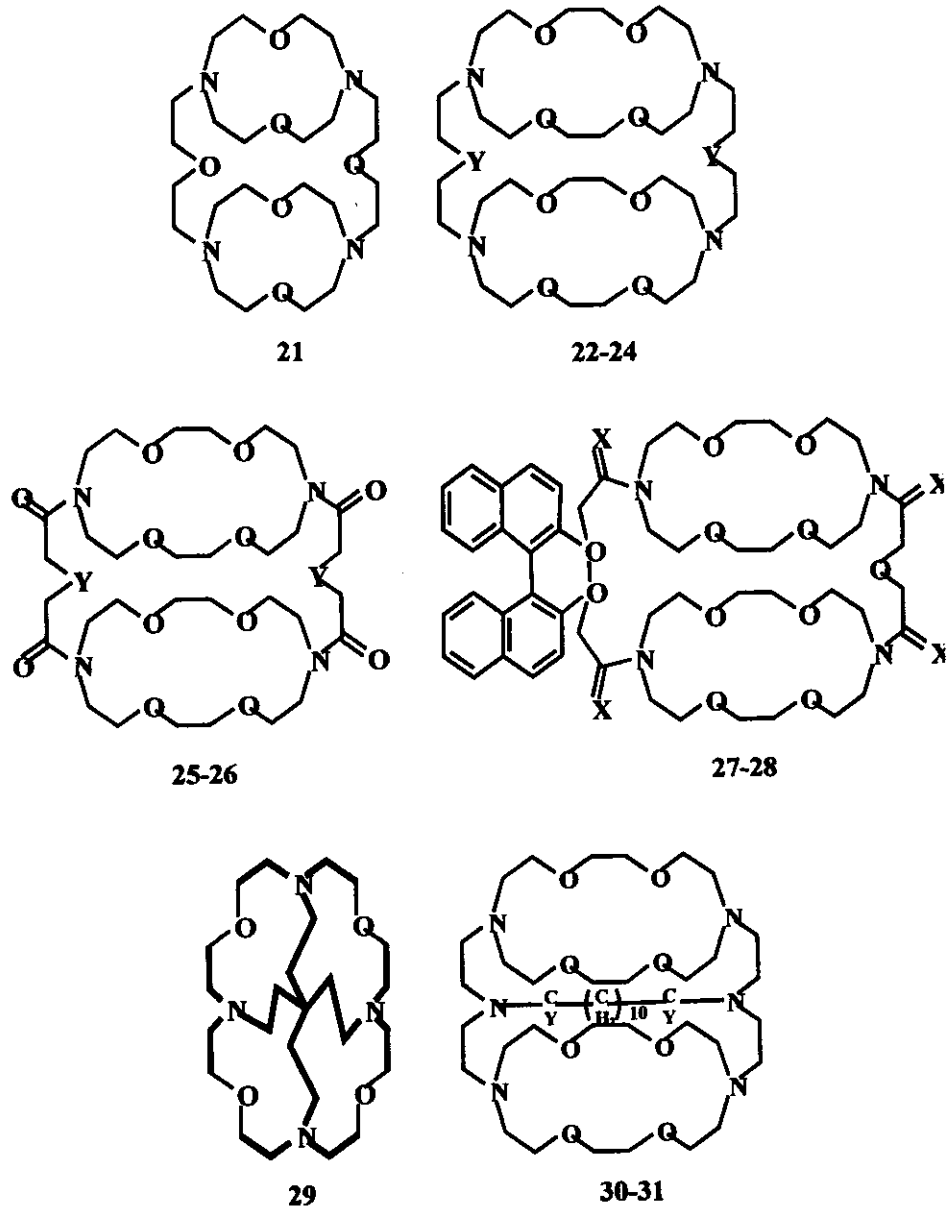

Fig. (1.3): 3- and 4-Cryptands

(22) Y = CH_2
(23) Y = O
(24) Y = NH
(25) Y = CH_2
(26) Y = O
(27) X = H_2
(28) X = O
(30) Y = O
(31) Y = H_2

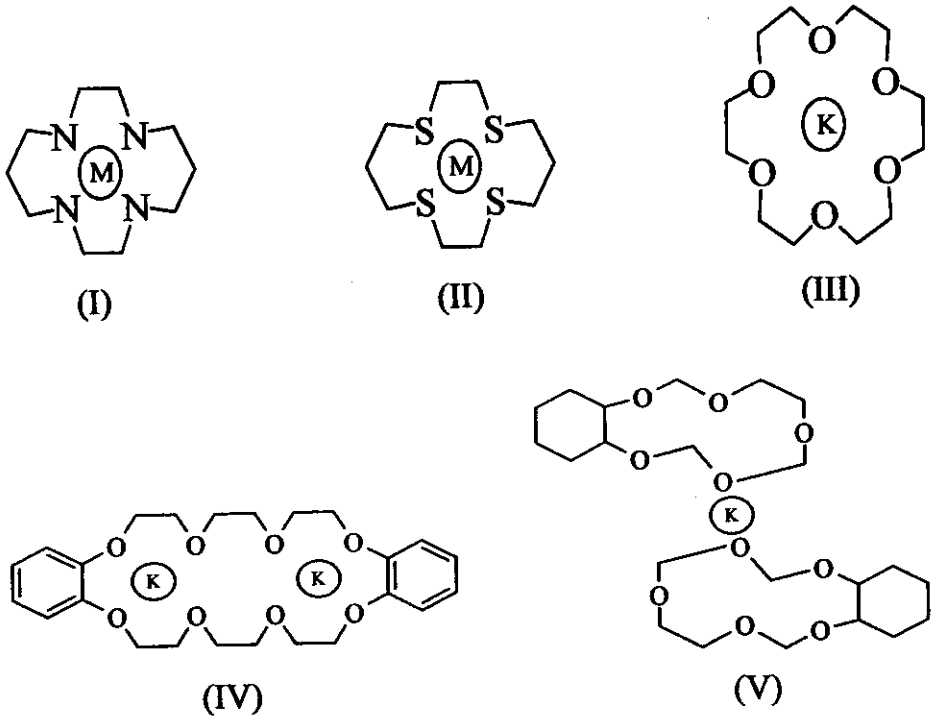

Fig. (1.4): Simplified structures of some crown ether complexes.

The study of organic compounds as corrosion inhibitors has both scientific and technological significance. Corrosion scientists and engineers have shown a great deal of interest in the study of macrocyclic compounds as corrosion inhibitors in recent years owing to their significant corrosion properties for industrial metals and alloys [143, 144].

A. T. panidi [145] investigated the corrosion behavior of Cu in accelerated testes and of Pb in lubricating oil in presence of different types of crown ether. It was found that the corrosion was decreased depending on the effectiveness of crown ethers as corrosion inhibitors and the length of the alkyl substituent on the ring of crown ethers reaching maximum for Cu constituents.

The corrosion problems of wet lime/limestone systems used for flue-gas desulphurization (FGD) in thermal power plants is of great concern [146]. The frequent variations in the acidity, and the chloride and fluoride ion concentrations experienced by the system, often cause major corrosion failure and pose a serious threat to the structural materials. The currently used materials (mostly type 316L stainless steel) seem to be effective but are not satisfactory as they often fail to meet their life expectancy. The study intends to evaluate the influence of 2-mercapto-benzothiazolyl disulfide (MBTDS) and 2-mercapto

benzimid az~olyl disulfide (MBIDS) on the localized corrosion of 316L stainless steel in a simulated (FGD) environment by performing cyclic anodic polarization measurements. Both (MBTDS) and (MBIDS) were found to be effective in the breakdown and pit protection potential thereby, improving the material's performance. The possible mode of adsorption and the way in which the inhibitors prevent the attack of the passive film of chloride ions present in the environment are discussed in detail. The present study concludes that both (MBTDS) and (MBIDS) are effective inhibitors for FGD systems.

2-Mercaptobenzothiazole and 2-amino-5-mercapto-1,3,4-thiadiazole control the corrosion of 304 stainless steel in 1.0 M H_2SO_4 solution by using weight loss, polarization resistance, SEM and Auger electron spectroscopy techniques [147]. Inhibition efficiency increases with increasing concentration and decreases with rising temperature (from 20 to 40 °C). Various corrosion parameters like Tafel slopes, corrosion rate, and heat of adsorption and activation energy were calculated. 2-Mercaptobenzothiazole is chemisorbed on the surface of 304SS whereas 2-amino-5-mercapto-1, 3, 4-thiadiazole is physically adsorbed. Both the studied compounds are cathodic inhibitors.

Macrocyclic compounds constitute a potential class of corrosion inhibitors [148]. In an attempt to develop effective corrosion inhibitors, four macrocyclic compounds (MOAT, BMOAT, OAH and BOAH) were synthesized by condensing o-ethylene and o-phenylene diamines with ethylacetoacetate and succinic acid. Their inhibiting action was evaluated on corrosion of mild steel in HCl and H_2SO_4 by weight loss and potentiodynamic polarization methods. A macrocyclic compound derived by condensing o-ethylene diamine with ethylacetoacetate exhibited best performance by giving IE of 98 percent at 500ppm concentration. The potentiodynamic polarization studies revealed that the tested compounds are either mixed type or predominantly cathodic inhibitors. IE of all the investigated compounds increased significantly on addition of a small concentration of KI in both acids due to synergism.

The effect of 4-amino-5H-3-mercapto1,2,4-triazole, 4-amino-5-methyl-3-mercapto-1,2,4-triazole and 4-amino-5-ethyl-3-mercapto-1,2,4-triazole as inhibitor were evaluated for the austenitic (grade 304) stainless steel in aqueous H_2SO_4 solutions at 298, 308, and 318 K using the weight loss, electrochemical polarization, potential decay, and electron microscopy data [149]. The three mercaptotriazoles are cathodic inhibitors that stimulate the anodic reaction of stainless steel, but tend to destabilize a passive film formed at the anodic

potentials. The corrosion inhibition is 93-96%, and increases with the higher temperature and the inhibitor concentration tested in the 100-800 ppm range.

A study has been made of the surface-active substances representing linear polyesters (polyethlenoxides) and their cyclic analogs (crown ethers) intended for use as corrosion inhibitors and stabilizers of the electrical characteristics of chemical storage cells [150]. The proposed surface-active substances belong to organic compounds whose molecules possess excess electrons localized at oxygen atoms, and which are capable of adsorption involving formation of hydrogen bonds, thus stabilizing the processes at the electrodes of storage cells. Having a larger polyester ring, crown ethers are capable of interacting with metal ions to produce complex associates, which increases their efficiency as surface-active substances and corrosion inhibitors. Using polyethlenoxides and their cyclic analogs in chemical storage cells with Zn and Cd anodes permits stabilization of their characteristics after secondary operation and after prolonged storage. In particular, the Zn corrosion rate in Ag-Zn storage cells decreases by a factor 2-3, and the operating life of Ag-Zn and Ag-Cd cells increases by a factor 1.5-2.

The influence of 4-amino-5-mercapto-3 n-propyl-1-2-4 triazol (AMPT) on corrosion and hydrogen permeation through mild steel in 0.5M H_2SO_4 and 1M HCl has been studied using weight loss measurements and various electrochemical techniques [151]. AMPT is found to be more inhibitive in H_2SO_4 than HCl. Potentiodynamic polarization studies clearly prove the fact that this compounds behaves as a mixed inhibitors, but predominantly as a cathodic inhibitor. Hydrogen permeation studies and AC impedance measurements also indicate an improved performance of the compound in H_2SO_4. The adsorption of this compound on the mild steel surface obeys Timken's adsorption isotherm.

2-undecane-5-mercapto-1-oxo-3, 4-diazole (UMOD), 2-heptadecane-5-mercapto-1-oxa-3, 4-diazole (HMOD) and 2-decane-5-mercapto-1-oxa-3, 4-diazole (DMOD) were synthesized in the laboratory and their influence on the inhibition of corrosion of mild steel in 1N HCl and 1N H_2SO_4 was investigated by weight loss and polarization techniques [152]. The inhibition efficiency of these compounds was found to vary with concentration, temperature and immersion time. Good inhibition efficiency was evidenced in both acid solutions, remaining high (> 90 %) even at the concentration of 250 ppm. The adsorption of compounds on the steel surface of both acids was found to obey Timken's isotherm. The values of E^*_a and ΔG_{ads} indicated physical adsorption on

mild steel surface. The potentiodynamic polarization data have shown that compounds studied are mixed type inhibitors.

2-Methyl benzoazole and 2-mercaptobenzoazole derivatives were investigated as corrosion inhibitors for the type 304 stainless steel in 2M H_2SO_4 solution using weight loss, gasometry, and alternating current (AC) impedance techniques [153]. Effect of immersion time and temperature were studied. The observed inhibition efficiency was found to depend on the heteroatom and type of side group. The efficiency of 2-methyl benzoselenazole (MBS), 2-mercaptobenzo~ imidazole (CBI), and 2-mercaptobenzothiazole (CBT) were independent of immersion time. However, MBS presented an efficiency of~90% at 45°C and caused a decrease in the activation energy of the corrosion process. Similarly, CBI and CBT had high efficiencies that remained almost unchanged at temperatures between 25°C and 55°C, but their activation energies increased slightly compared to that in their absence. Chemisorption of inhibitor molecules was used to explain the results of this study.

Inhibition efficiencies of 2-mercaptobenzoazole and 2-methylbenzoazole, containing nitrogen, sulfur, oxygen, and selenium atoms, on the corrosion of 304 stainless steel in 2M sulphuric acid and 3M HCl have been investigated [154]. The study was conducted using weight loss, gasometry, and polarization methods. It was shown that some of the compounds tested provide 90 % inhibition efficiency at a concentration of $5X10^{-4}$ M and that the efficiency depends on the heteroatom and decreases in the order Se > S > N > O. These inhibitors were more efficient in H_2SO_4 than in HCl whereas the opposite is true for inhibitors with nitrogen alone. Adsorption isotherms were fitted to the experimental findings and some thermodynamics functions were obtained.

2-Mercaptopyrimidine (2-MP) is a non-poisonous material [155]. It has been studied as a corrosion inhibitor, such as the inhibition of Cu in H_2SO_4 [156], carbon and low-alloy steels in H_2SO_4 [157] and Al alloy in chloride solution [158]. But little work appears to have been done on the inhibition of low carbon steel (LCS) in H_3PO_4 solution. Polarization and weight loss studies by Lin Wang [159] showed that 2-mercaptopyrimidine is effective for the inhibition of low carbon steel over a wide concentration range of aqueous phosphoric acid (H_3PO_4) solutions. The inhibition retards the anodic and cathodic corrosion reactions with emphasis on the former.